Faraday polarisation mode conversion in semiconductor waveguides incorporating periodic garnet claddings

David C. Hutchings[a], Cui Zhang[a], Barry M. Holmes[a], Prabesh Dulal[b], Andrew D. Block[c], and Bethanie J. H. Stadler[bc]

[a]School of Engineering, University of Glasgow, Glasgow G12 8LS, Scotland, U.K.
[b]Chemical Engineering and Materials Science, University of Minnesota, Minneapolis, Minnesota 55455, U.S.A.
[c]Electrical Engineering, University of Minnesota, Minneapolis, Minnesota 55455, U.S.A.

ABSTRACT

We report on our progress towards the integration of nonreciprocal optical elements in, for example, an integrated optical waveguide isolator on conventional semiconductor photonic platforms. Our approach uses an evanescent interaction with a magneto-optic iron garnet upper cladding. Specifically, cerium- and bismuth- substituted yttrium and terbium iron garnets were investigated. Device fabrication incorporates RF sputtering, mask lift-off to form a grating for a quasi-phase-matched interaction and thermal anneal. A non-reciprocal polarisation-mode conversion was observed.

Keywords: optical isolators, magneto-optics, waveguide devices, integrated photonics

1. INTRODUCTION

The nonreciprocal optical effect of Faraday rotation is widely exploited in optical isolators to suppress back-reflections to protect optical sources and other devices from injection noise, or in optical circulators to route counter-propagating signals in a single physical channel to different ports. To date, these devices are assembled from bulk components. For example, an optical isolator normally consists of two linear polarisers set at 45° to each other, a bulk or normal-incidence thin film magneto-optic crystal (usually from the iron garnet family) and a permanent magnet. The consequence of using bulk components to build optical systems is that the assembly and alignment of the components limits production volumes, affects reproducibility and yield, and becomes a major part of the overall manufacturing cost. Conversely, photonic integration has proved technically successful in developing techniques for combining multiple optical devices onto a single chip with the benefits of added functionality, and reduction in costs, arising from the replacement of manual assembly and alignment of individual components with lithographic techniques.

There are a number of challenges to be overcome in the implementation of magneto-optic elements in opto-electronic integrated circuits (OEIC) or photonic integrated circuits (PIC).[1,2] At near-IR wavelengths the iron garnets are overwhelmingly best suited as magneto-optic materials due to the comparatively large imaginary off-diagonal terms in the dielectric tensor whilst retaining a low optical loss. The first challenge is a consequence of the typical refractive indices for garnets being far smaller than the guiding layer in semiconductor OEIC/PICs. Butt-coupling of such heterogeneous materials, which would be technologically challenging anyway, will result in interface (Fresnel and mode-mismatch) reflections, which are obviously undesirable in an optical isolator. An alternative configuration, which is becoming widely deployed in integrated magneto-optics, is to use the evanescent interaction with a magneto-optic medium as an upper cladding to a semiconductor guiding layer.[1,3] This cladding approach has also been used with the nonreciprocal phase-shift obtained through the transverse magneto-optic Kerr effect with direct bonding,[4,5] adhesive bonding[6,7] and deposition[8] on silicon-on-insulator wafers.

Further author information: (Send correspondence to D.C.Hutchings)
D.C.Hutchings: E-mail: David.Hutchings@glasgow.ac.uk, Telephone: +44 (0)141 330 6026

The second challenge to the facilitation of optical isolation by Faraday rotation in an integrated format is that, while there are solutions to provide polarisers, or polarisation mode splitting, with a polarisation orientation in-plane or normal to the wafer, it is not straightforward to do this for an arbitrary (in this case 45°) orientation. One solution to this is to incorporate a reciprocal polarisation mode converter (R-PMC), which has the functionality of a birefringent waveplate, based on an asymmetric profile waveguide.[7,9–13] The required reciprocal polarisation mode conversion can be achieved either with a quarter-waveplate with optic axis at 45° or a half-waveplate with an optic axis at 22.5° equivalents. The physical realisation of an effective optic axis at 45° in a guided wave format can only be approached asymptotically and therefore the half-waveplate with an effective optic axis at 22.5° offers a more practical solution.[14]

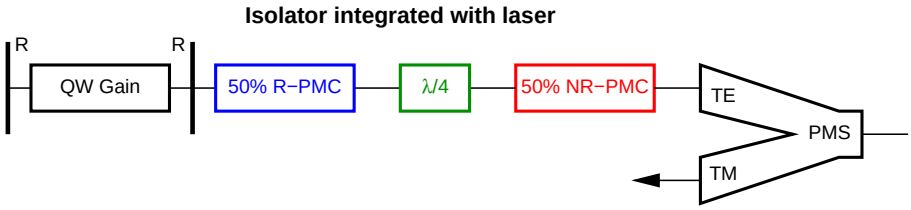

Figure 1. Building blocks for integrated waveguide devices. The nonreciprocal polarisation mode converter section is shown in red, the universal 3 dB reciprocal polarisation mode converter section is shown in blue, and a fixed differential phase retarders is shown in green. Additional polarisation discrimination may be provided by polarisation mode splitters (PMS) and anisotropic gain in a quantum well laser.

Fig. 1 shows a schematic of a possible implementation of an integrated optical isolator based on Faraday rotation. The final polarisation mode splitter (PMS) is only necessary should there be significant TM-polarised reflected light in the system. The quantum-well laser provides the other polarisation discrimination as it emits TE-polarised light from the heavy-hole transition, yet is transparent to TM-polarised light at the lasing wavelength. The combination of a nonreciprocal polarisation mode converter and a reciprocal polarisation mode conversion cancel each other in the forward direction, but provide a cumulative TE- to TM-polarisation mode conversion in the reverse. The additional quarter-waveplate ensures the correct phase between the polarisation modes with the half-waveplate R-PMC design.

The third challenge to be able to exploit Faraday rotation in an integrated format is a consequence of the planar format of OEIC/PICs which introduces a birefringence into the waveguides, and will form the principal subject for this paper. Faraday rotation is an example of coherent mode-conversion where the direction of energy transfer is phase dependent. A mismatch in modal phase velocities places a constraint on the extent of the energy transfer between modes. This phase-matching requirement was first recognised in optics for optical frequency generation. Quasi-phase-matching (QPM) is a technique where the medium is spatially modified periodically to compensate for a phase velocity mismatch and ensure a monotonic flow of energy between the modes. The most widely exploited QPM technique is domain reversal[15] achieved by stacking plates, by dopant diffusion, by electric-field poling, or by growth on orientation-patterned substrates. More generally, the extent of the monotonic modal conversion is determined by magnitude of the appropriate order (normally first-order) spatial Fourier coefficient.[16] Quasi-phase-matching can also be applied to nonreciprocal polarisation mode conversion. Initial demonstrations were on a planar waveguide format with mode confinement in the vertical direction only. Tien et al used a serpentine current strip to provide a periodically reversed applied magnetic field.[17] Post-deposition laser annealing has also been employed to spatially modulate the net magneto-optic coefficient.[18,19]

In this paper, we demonstrate a fabrication approach for nonreciprocal mode conversion in semiconductor waveguides where the upper cladding contains magneto-optic iron garnets and hence interacts through the mode evanescent tail. The mode conversion is phase-matched using a quasi-phase-matching approach where lithography of the magneto-optic iron garnet provides periodic segments with length and separation determined by the coherence length of the modal conversion process.

2. FABRICATION

The substantive mis-match in thermal expansion between garnets and semiconductor substrates can be accommodated by restricting the precursor deposition to sufficiently small segments, such as the micron scale width

of optical waveguide cores or claddings, prior to crystallisation under annealing.[20] A lift-off process has been developed in order to pattern the deposited amorphous garnet precursor using a PMMA resist mask written using e-beam lithography.[21] A bi-layer PMMA resist mask was employed; the higher molecular weight of the upper layer results in a slightly thinner opening at the top of the mask, leading to an overhang profile and thus avoiding sidewall deposition. Careful optimisation of the e-beam writing parameters results in both the size of the desired features (in this case widths of between 200 nm and 2 μm with lengths from 10 μm to several millimetres), as well as the required overhanging sidewall profile of the mask, to be obtained reproducibly. The garnet precursor was deposited using RF sputtering with argon plasma with 20.4 sccm Ar flow. The Fe target was sputtered at 220 W while the Y or Tb targets were typically sputtered at 120 W. The deposition was performed with a 2.0 sccm oxygen flow and the chamber pressure was held at a constant 6.0 mtorr.

The PMMA mask is then removed and a rapid thermal anneal is performed under flowing oxygen (10 slpm) typically at 850°C or 900°C for 120 s. A uniform morphology is obtained at anneal temperatures of 800–850°C, comparable to garnet waveguides on SiO_2 formed by wet-etch, which had measured optical losses of ∼1 dB/mm at a wavelength of 1.55 μm.[20] A typical garnet segment fabrication is shown in fig. 2 which shows Ce:YIG on a MgO seed layer before anneal (top), and after the first (middle) and second (bottom) anneals. Note that the actual layer thickness is much reduced from the nominal deposition on open areas due to the angular restriction of deposition due to the PMMA mask. The sputtered precursor of Ce:YiG deposition on silicon normally does not form the garnet phase under rapid thermal anneal, but the introduction of a seed layer, such as at least 15 nm thick YIG layer, can result in Ce:YIG forming the desired garnet phase.[8,22] Additional information about the crystal structure of segmented regions following anneal could be obtained using electron backscatter diffraction (EBSD); we find that there is at least partial crystallisation of Ce:YIG (to a polycrystalline garnet) when a MgO seed layer is used.

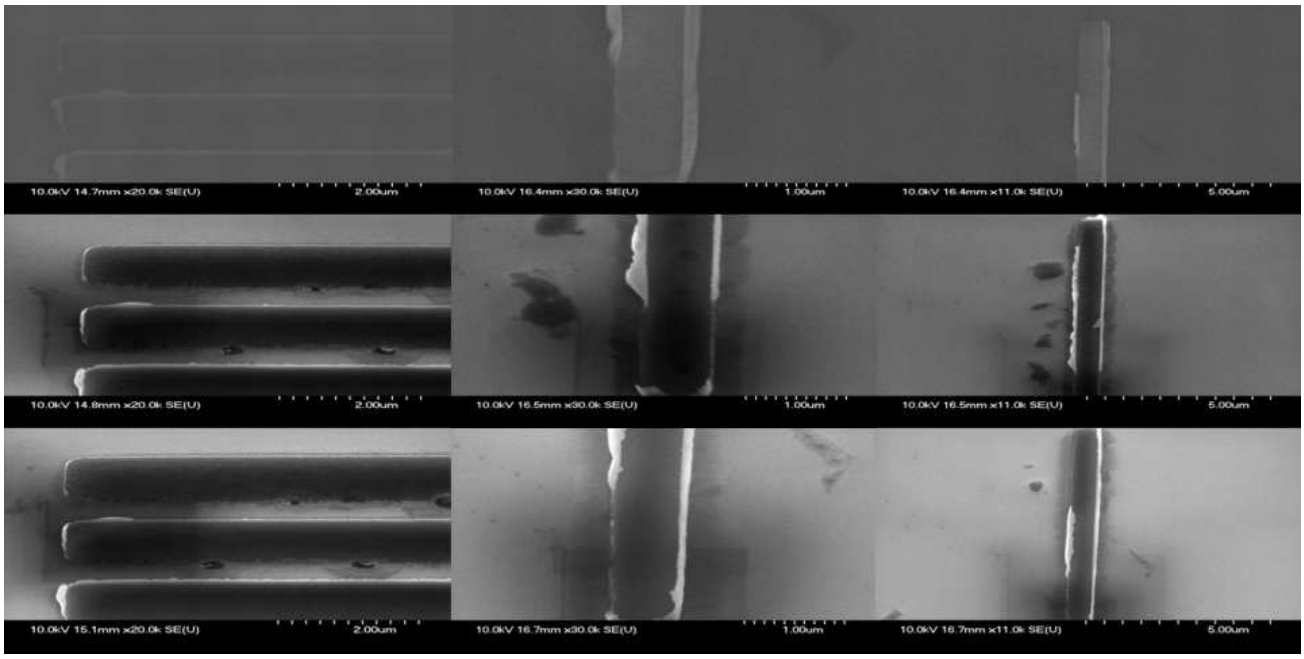

Figure 2. SEMs of segments of Ce:YIG (300 nm nominal thickness on open area) on MgO seed layer (100 nm nominal thickness on open area) deposited on silicon-on-insulator. Top SEM shows the precursor following lift-off of the PMMA mask, middle and lower SEMs show the segment after the first and second anneal at 900°C.

Whilst the use of an appropriate seed layer can aid the crystallisation of cerium-substituted YIG into the garnet phase, it comes at a cost of significantly reducing the modal overlap of the mode's evanescent tail with the film of the higher magneto-optic effect,[21] even when taking a minimal seed layer thickness for the promotion of crystallisation. Therefore, there has been recent renewed interest in substituted terbium iron garnets,[23] such as Bi:TIG and Ce:TIG, which generally do not require a seed layer when deposited by sputtering onto

silicon for the garnet phase to form under rapid thermal annealing. Use of terbium iron garnets does provide another fabrication approach to quasi-phase-matching of Faraday rotation. The substituted garnets Bi:TIG and Ce:TIG have the opposite sign of magneto-optic effect compared to TIG at a wavelength of 1550 nm. Therefore alternating segments of TIG and substituted TIG will have a larger first-order spatial Fourier component and hence an enhanced Faraday rotation in comparison to each garnet individually, whilst keeping the refractive index of the cladding close to constant. Fig. 3 shows the aligned cladding segments with two stages of lift-off mask and deposition. The first deposited segments are of Bi:TIG, which have been annealed, and the second deposited segments are of TIG: the SEM on the left is prior to the second anneal and on the right after the second anneal, crystallising the TIG segments.

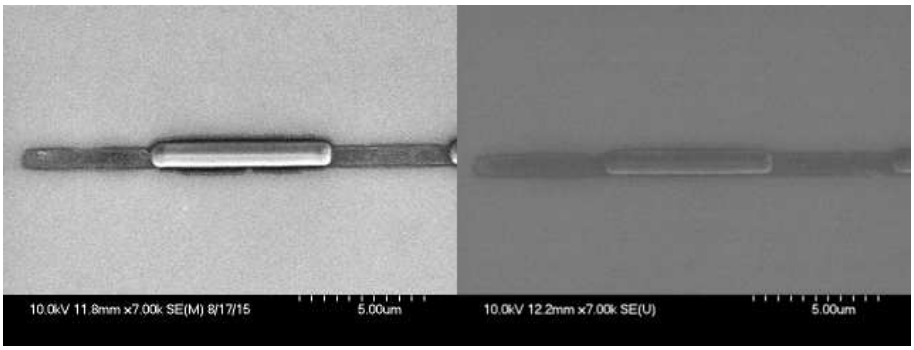

Figure 3. SEMs following two deposition and lift-off stages with mask realignment. The first layer is Bi:TIG (annealed) and the second layer is TIG shown before (left) and after (right) anneal.

Following the annealing, silica waveguide masks aligned to the iron garnet segments are written by electron-beam lithography of spun HSQ, with a range of widths, typically from 500 to 1100 nm. Silicon-core waveguides are formed with a chlorine-based etch in an ICP etcher. Fig. 4 (left) shows an example of such a fabricated waveguide. In order to reduce the upper cladding refractive index variation some samples are coated with silicon nitride, which has a similar refractive index to garnet, prior to etching (resultant waveguides shown in fig. 4 middle and right). This will reduce the possibility of Bragg scattering, and will mitigate against reciprocal polarisation mode conversion caused by the asymmetry of any small unintended lateral offset between the garnet and the waveguide (periodic loading).

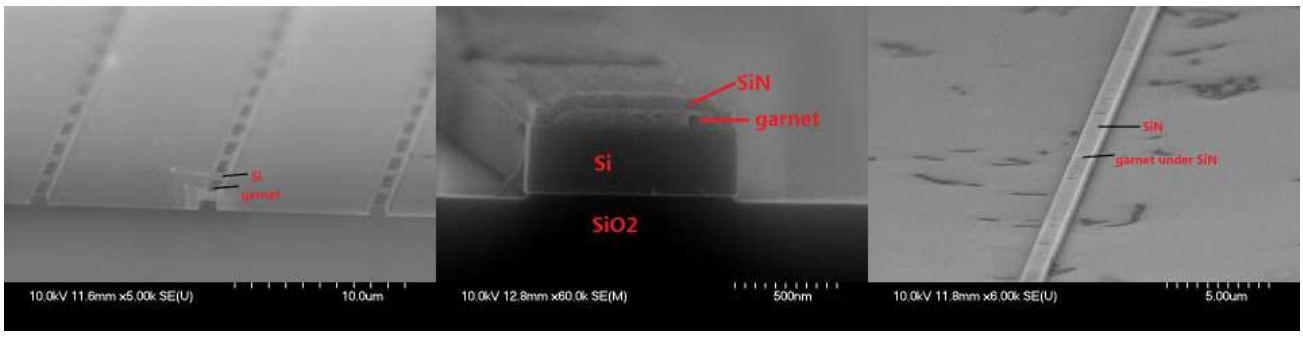

Figure 4. SEMs of fabricated silicon-on-insulator waveguides with a periodic upper cladding containing iron garnet segments. Left shows a garnet clad waveguide without additional layers. Middle and right show samples which have been over-clad with silicon nitride prior to etching.

3. OPTICAL CHARACTERISATION

The optical characterisation of the fabricated waveguides was performed by end-fire coupling of a tunable 1550 nm laser. For the results shown here, the light is launched as linear TE-polarisation throughout. The samples consist of a 500 nm thick silicon guiding layer on SiO_2. The segmented iron garnet cladding consists of either Bi:TIG or Ce:TIG, which have then been over-clad with silicon nitride. The waveguide lengths are of the order of a

millimetre and there is a range of segment lengths and gaps of the order of 10 μm, corresponding to the calculated coherence length between the fundamental TE- and TM-polarised modes.[14]

The first set of measurements presented here show the relative fraction of TM-polarised light obtained by using a polarising beam splitter cube at the waveguide output. Initially this was performed for the as-fabricated samples, and then repeated after saturating the magnetisation with a longitudinal magnetic field (>1 kOe). Hence, the observed longitudinal magneto-optic effect is due to the remanant magnetisation in this ferromagnetic medium. The left figure shows this polarisation fraction for Bi:TIG in fig. 5, and for Ce:TIG in fig. 6. For the Bi:TIG clad waveguide, there is a peak polarisation mode conversion at λ=1532 nm in the unsaturated state, indicating some reciprocal polarisation mode conversion most likely due to a small unintended offset between lithography masks. This peak mode conversion is substantially enhanced following magnetic saturation. For the Ce:TIG clad waveguide, there is no discernible polarisation mode conversion in the unsaturated state, with a substantive peak developing in either direction of longitudinal magnetic saturation at λ=1511 nm. The resonant nature of the mode-conversion is due to the phase-matching criteria and different QPM periods will correspond to different peak wavelengths.

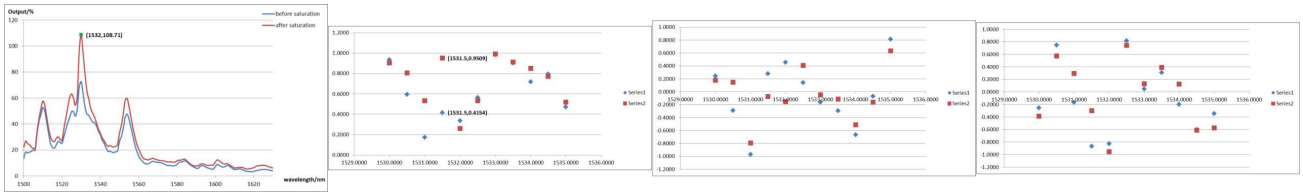

Figure 5. Wavelength dependence of the polarisation state of the transmitted light with a TE-polarised input around 1550 nm for a silicon waveguide with periodic Bi:TIG upper cladding. The left plot shows the relative power corresponding to TM-polarisation before and after longitudinal magnetic saturation. The 3 plots on the right show the three Stokes parameters (S_1, S_2, S_3) respectively of the output polarisation state measured with a polarimeter for TE-polarised input for the opposite directions of longitudinal magnetic saturation.

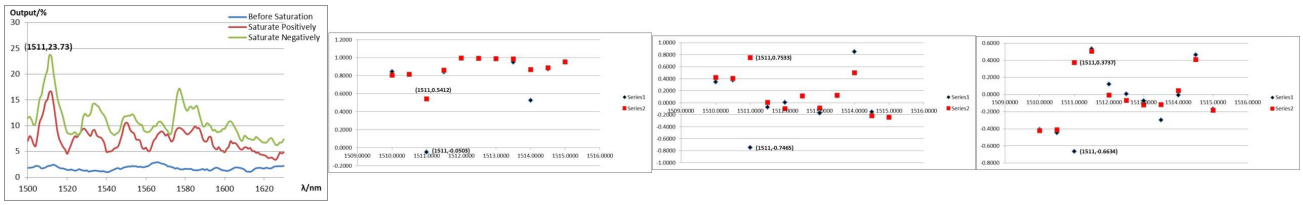

Figure 6. Wavelength dependence of the polarisation state of the transmitted light with a TE-polarised input around 1550 nm for a silicon waveguide with periodic Ce:TIG upper cladding. The left plot shows the relative power corresponding to TM-polarisation before and after longitudinal magnetic saturation in both directions. The 3 plots on the right show the three Stokes parameters (S_1, S_2, S_3) respectively of the output polarisation state measured with a polarimeter for TE-polarised input for the opposite directions of longitudinal magnetic saturation.

The polarisation state of the transmitted light is investigated further by analysing it with a polarimeter. The three plots on the right of figs. 5 and 6 show the three Stokes parameters (S_1, S_2, S_3) respectively for both longitudinal directions of magnetic saturation (equivalent to reversing the sample whilst maintaining similar coupling conditions) with a TE-polarised input. In both cases there is a divergence between the transmitted polarisation state limited to a range of wavelengths corresponding to the polarisation mode conversion peak observed on the left-hand plot. For the Bi:TIG clad waveguide the output polarisation at λ=1531.5 nm is close to linear TE-polarised ($S_1 \approx 1$) for the saturation direction corresponding to the red squares, yet close to circular polarisation ($S_3 \approx -1$) for the opposite saturation direction, corresponding to blue diamonds. For the Ce:TIG clad waveguide we observe that there is a change in sign in the S_2 and S_3 Stokes parameters at λ=1511 nm, indicating that both the orientation of the major axis and the sense of the ellipse have reversed for the transmitted polarisation state on reversing the longitudinal magnetic saturation.

4. CONCLUSIONS

We have presented a lift-off technique which, along with multiple target RF-sputtering of iron garnets followed by a rapid thermal anneal, facilitates the fabrication of garnet segments on a silicon surface. These are used to provide a quasi-phase-matched polarisation mode conversion by evanescent interaction with a spatially periodic magneto-optic upper cladding in silicon-on-insulator optical waveguides for the 1550 nm telecommunications band. We show the effect on TE-polarised end-fire coupled light into waveguides with either Bi:TIG or Ce:TIG cladding segments, over-clad with silicon nitride. It is shown that the transmitted polarisation state is substantially altered by the direction of longitudinal magnetisation over a limited phase-matching defined wavelength window, thus demonstrating the degree of nonreciprocal polarisation mode conversion required for an integrated optical isolator.

ACKNOWLEDGMENTS

This research was sponsored as a World Materials Network by the Engineering and Physical Sciences Research Council (EP/J018708/1) and the National Science Foundation (DMR-1210818). The authors acknowledge the valuable support of sample fabrication by the technical staff of the James Watt Nanofabrication Centre. The authors also thank the Minnesota Nanofabrication Center and the Characterization Facility, both of which work under partial support from the NSF National Nanotechnology Infrastructure Network (NNIN).

REFERENCES

[1] D. C. Hutchings, "Prospects for the implementation of magneto-optic elements in optoelectronic integrated circuits: a personal perspective (invited)," *J. Phys. D* **36**, pp. 2222–2229, 2003.

[2] B. J. H. Stadler and T. Mizumoto, "Integrated magneto-optical materials and isolators: A review," *IEEE Photon. J.* **6**, p. 0600215, 2014.

[3] H. Yokoi, T. Mizumoto, and H. Iwasaki, "Nonreciprocal TE-TM mode converter with semiconductor guiding layer," *Electronics Letters* **38**, pp. 1670–1672, 2002.

[4] Y. Shoji, T. Mizumoto, H. Yokoi, L.-W. Hsieh, and J. R. M. Osgood, "Magneto-optical isolator with silicon waveguides fabricated by direct bonding," *Appl. Phys. Lett.* **92**, p. 071117, 2008.

[5] Y. Shoji, M. Ito, Y. Shirato, and T. Mizumoto, "Mzi optical isolator with si-wire waveguides by surface-activated direct bonding," *Optics Express* **20**, pp. 18440–18448, 2012.

[6] S. Ghosh, S. Keyvavinia, W. V. Roy, T. Mizumoto, G. Roelkens, and R. Baets, "Ce:yig/silicon-on-insulator waveguide optical isolator realized by adhesive bonding," *Optics Express* **20**, pp. 1839–1848, 2012.

[7] S. Ghosh, S. Keyvavinia, Y. Shirato, T. Mizumoto, G. Roelkens, and R. Baets, "Optical isolator for te polarized light realized by adhesive bonding of ce:yig on silicon-on-insulator waveguide circuits," *IEEE Photonics Journal* **5**, p. 6601108, 2013.

[8] L. Bi, J. Hu, P. Jiang, D. H. Kim, G. F. Dionne, L. C. Kimerling, and C. A. Ross, "On-chip optical isolation in monolithically integrated non-reciprocal resonators," *Nature Photonics* **5**, pp. 758–762, 2011.

[9] V. P. Tzolov and M. Fontaine, "A passive polarization converter free of longitudinally-periodic structure," *Optics Commun.* **127**, pp. 7–13, 1996.

[10] J. Z. Huang, R. Scarrmozzino, G. Nagy, M. J. Steel, and R. M. Osgood, Jr., "Realization of a compact and single-mode optical passive polarization converter," *IEEE Photon. Tech. Lett.* **12**, pp. 317–319, 2000.

[11] B. M. Holmes and D. C. Hutchings, "Realisation of novel low-loss monolithically integrated waveguide mode converters," *IEEE Photonics Tech. Lett.* **18**, pp. 43–45, 2006.

[12] L. M. Augustin, J. J. G. M. van der Tol, E. J. Geluk, and M. K. Smit, "Short polarization converter optimized for active-passive integration in InGaAsP-InP," *IEEE Photon. Technol. Lett.* **19**, pp. 1673–1675, 2007.

[13] B. M. Holmes, M. A. Naeem, D. C. Hutchings, J. H. Marsh, and A. E. Kelly, "A semiconductor laser with monolithically integrated dynamic polarization control," *Optics Express* **20**, pp. 20545–20550, 2012.

[14] D. C. Hutchings and B. M. Holmes, "A waveguide polarisation toolset design based on mode-beating," *IEEE Photonics Journal* **3**, pp. 450–461, 2011.

[15] J. A. Armstrong, N. Bloembergen, J. Ducuing, and P. S. Pershan, "Interactions between light waves in a nonlinear dielectric," *Phys. Rev.* **127**, pp. 1918–1939, 1962.

[16] D. C. Hutchings and T. C. Kleckner, "Quasi-phase-matching in semiconductor waveguides using intermixing: optimisation considerations," *J. Opt. Soc. Am. B* **19**, pp. 890–894, 2002.

[17] P. K. Tien, R. J. Martin, R. Wolfe, R. C. L. Craw, and S. L. Blank, "Switching and modulation of light in magneto-optic waveguides of garnet films," *Appl. Phys. Lett.* **21**, pp. 394–396, 1972.

[18] R. Wolfe, J. Hegarty, J. J. F. Dillon, L. C. Luther, G. K. Celler, and L. E. Trimble, "Magneto-optic waveguide isolators based on laser annealed (Bi, Ga) YIG films," *IEEE Trans. Magn.* **21**, pp. 1647–1650, 1985.

[19] K. Ando, T. Okoshi, and N. Koshizuka, "Waveguide magneto-optic isolator fabricated by laser annealing," *Appl. Phys. Lett.* **53**, pp. 4–6, 1988.

[20] S.-Y. Sung, A. Sharma, A. Block, K. Keuhn, and B. J. H. Stadler, "Magneto-optical garnet waveguides on semiconductor platforms: Magnetics, mechanics and photonics," *J. Appl. Phys.* **109**, p. 07B738, 2011.

[21] D. C. Hutchings, B. M. Holmes, C. Zhang, P. Dulal, A. D. Block, S.-Y. Sung, N. C. A. Seaton, and B. J. H. Stadler, "Quasi-phase-matched faraday rotation in semiconductor waveguides with a magnetooptic cladding for monolithically integrated optical isolators," *IEEE Photon. J.* **5**, p. 6602512, 2013.

[22] A. D. Block, P. Dulal, B. J. H. Stadler, and N. C. A. Seaton, "Growth parameters of fully crystallized yig, bi:yig, and ce:yig films with high faraday rotations," *IEEE Photon. J.* **6**, p. 0600308, 2014.

[23] P. Dulal, A. Block, H. A. Haldren, D. C. Hutchings, and B. J. H. Stadler, "Effects of different seedlayers on the magneto-optic properties of rare earth iron garnets grown on semiconductor substrates," in *Joint MMM-Intermag Conference, San Diego CA*, p. FI05, IEEE Magnetics Society, 2016.